

The chemical chaperone 4-phenylbutyrate inhibits adipogenesis by modulating the unfolded protein response^S

Sana Basseri,* Šárka Lhoták,* Arya M. Sharma,[†] and Richard C. Austin^{1,*}

Department of Medicine,* McMaster University, St. Joseph's Healthcare Hamilton and the Henderson Research Centre, Hamilton, Ontario, L8N 4A6, Canada; and Royal Alexandra Hospital,[†] Edmonton, Alberta, T5H 3V9, Canada

Abstract Recent studies have shown a link between obesity and endoplasmic reticulum (ER) stress. Perturbations in ER homeostasis cause ER stress and activation of the unfolded protein response (UPR). Adipocyte differentiation contributes to weight gain, and we have shown that markers of ER stress/UPR activation, including GRP78, phospho-eIF2 α , and spliced XBP1, are upregulated during adipogenesis. Given these findings, the objective of this study was to determine whether attenuation of UPR activation by the chemical chaperone 4-phenylbutyrate (4-PBA) inhibits adipogenesis. Exposure of 3T3-L1 preadipocytes to 4-PBA in the presence of differentiation media decreased expression of ER stress markers. Concomitant with the suppression of UPR activation, 4-PBA resulted in attenuation of adipogenesis as measured by lipid accumulation and adiponectin secretion. Consistent with these *in vitro* findings, female C57BL/6 mice fed a high-fat diet supplemented with 4-PBA showed a significant reduction in weight gain and had reduced fat pad mass, as compared with the high-fat diet alone group. Furthermore, 4-PBA supplementation decreased GRP78 expression in the adipose tissue and lowered plasma triglyceride, glucose, leptin, and adiponectin levels without altering food intake. Taken together, these results suggest that UPR activation contributes to adipogenesis and that blocking its activation with 4-PBA prevents adipocyte differentiation and weight gain in mice.—Basseri, S., Š. Lhoták, A. M. Sharma, and R. C. Austin. **The chemical chaperone 4-phenylbutyrate inhibits adipogenesis by modulating the unfolded protein response.** *J. Lipid Res.* 2009. 50: 2486–2501.

Supplementary key words ER stress • obesity • adipocyte differentiation • 3T3-L1

Obesity and excess body fat are well-known risk factors for diabetes and cardiovascular disease (1). Obesity rates have been increasing at an alarming rate, and the obesity epidemic is predicted to worsen given that 22 million children worldwide under the age of five are severely overweight (2). Recently, it has become evident that white adipose tissue is highly dynamic and plays major roles in energy balance and regulation. White adipose tissue also acts as an endocrine organ that carries out various physiological processes and secretes hormones, such as leptin and adiponectin, as well as inflammatory factors like MCP-1, IL-6, and TNF α into the circulation (3). Adipogenesis, the recruitment and conversion of a fibroblast-like preadipocyte into mature fat cells involves the process of adipocyte differentiation (3). In recent years, there has been significant progress in understanding adipocyte differentiation and adipose tissue expansion. Adipogenesis is triggered by a physiological need to increase the number of adipocytes when preexisting adipocytes reach a critical cell size (4). An increase in the number of cells through adipocyte differentiation (hyperplasia) and an increase in adipocyte size (hypertrophy) lead to adipose tissue expansion (5). The focus of this study was adipocyte differentiation, a highly regulated cellular process that results in

This work was supported in part by research grants to R.C.A. from the Heart and Stroke Foundation of Ontario (T-6146, NA-6024, and NA-6393) and the Canadian Institutes of Health Research (MOP-67116 and MOP-74477). Research funding from St. Joseph's Healthcare Hamilton is also acknowledged. R.C.A. is a Career Investigator of the Heart and Stroke Foundation of Ontario (CI-5959) and holds the Amgen Canada Research Chair in Nephrology. Dr. Austin and Dr. Sharma were funded by a Canadian Institutes of Health Research (CIHR)/Heart and Stroke Foundation of Canada (HSFC) Grant 116099. S.B. was supported by a Master's Studentship from the Heart and Stroke Foundation of Ontario.

Manuscript received 29 April 2009.

Published, JLR Papers in Press, May 21, 2009
DOI 10.1194/jlr.M900216-JLR200

Abbreviations: CHOP, C/EBP homologous protein; eIF2 α , α -subunit of eukaryotic translational initiating factor 2; ER, endoplasmic reticulum; GRP78, glucose-regulated protein of 78-kDa; HDAC, histone deacetylase; IRE1, inositol requiring enzyme 1; MDI, isobutylmethylxanthine dexamethasone and insulin; MEF, mouse embryonic fibroblast; 4-PBA, 4-phenylbutyric acid; PERK, PKR-like endoplasmic reticulum kinase; SREBP, sterol-regulatory element binding protein; UPR, unfolded protein response; XBP1, X-box binding protein 1.

¹To whom correspondence should be addressed.

e-mail: raustin@thrombosis.hhsr.org

^SThe online version of this article (available at <http://www.jlr.org>) contains supplementary data in the form of six figures.

Copyright © 2009 by the American Society for Biochemistry and Molecular Biology, Inc.

metabolically active adipocytes capable of synthesizing and secreting a number of hormones and cytokines (3, 6, 7).

There is some evidence suggesting that obesity may be a disease related to endoplasmic reticulum (ER) dysfunction (8–11). It has been reported that defective ER signaling in the obese state leads to the retention and accumulation of proteins that are normally susceptible to ER-associated degradation (8, 9). The oxidizing environment of the ER provides ideal conditions for membrane proteins as well as secretory proteins to fold into their native conformation (12). However, ER stress occurs when the homeostatic environment of the ER is disrupted due to adverse physiological conditions, such as nutrient deprivation, hypoxia, or viral infection, leading to the accumulation of unfolded or misfolded polypeptides in the ER lumen (9, 10, 13). The majority of cells cope with the increased ER load by activating the unfolded protein response (UPR), an integrated signal transduction pathway consisting of three distinct mediators, inositol requiring enzyme 1 (IRE1), PKR-like ER kinase (PERK), and activating transcription factor 6 (ATF6). Activation of these mediators leads to translation attenuation, clearance of misfolded proteins through ER-associated degradation, increased ER folding capacity, and the upregulation of ER chaperones that assist in protein folding (9).

The reasons for ER stress and UPR activation in the obese state are not fully understood. ER stress has been linked to conditions such as hyperinsulinemia (14) and hyperglycemia (10, 15), both of which can promote adipocyte differentiation and weight gain (1, 4). Furthermore, nutrient imbalance, excessive lipid storage, and insulin resistance in the hypertrophied adipocyte can lead to ER stress and UPR activation (5, 11). Several studies have reported that there is upregulation of ER stress markers such as GRP78 (glucose-regulated protein of 78-kDa), phospho-PERK, and phospho-eIF2 α (α -subunit of eukaryotic translational initiating factor 2) in adipose tissue, liver, and hypothalamus of obese mice, indicative of ER stress in these tissues (10, 14, 16–19). Recent human studies have also demonstrated increased ER stress in adipose tissue from both obese insulin-resistant subjects (20) and obese nondiabetic subjects (21). Furthermore, examination of liver and adipose tissues of obese subjects after weight loss provided evidence of reduced ER stress in these tissues (22). While a direct link between ER homeostasis and transcriptional regulation of metabolic genes such as C/EBP α in the context of fatty liver disease has been established (17, 23), the role of ER stress in adipogenesis and weight gain has not been fully explored. In a recent study, the PERK pathway was shown to be required for lipogenesis and adipogenesis (24). X-box binding protein 1 (XBP1), a transcription factor upregulated by ATF6 and spliced by the IRE1 pathway (25), and phosphorylation of eIF2 α , which occurs downstream of the PERK pathway, were shown to regulate lipogenesis in the liver (17, 26). However, little is known about the role of these UPR pathways in adipogenesis and adipose tissue biology. The ER of cells with a high secretory capacity, such as hepatocytes, plasma B cells, and pancreatic β cells, is well developed and ex-

panded in order to accommodate the flux of de novo proteins into the ER for folding and secretion (9). Since differentiating adipocytes are also highly secretory in nature and are metabolically active (3), we hypothesized that UPR activation and upregulation of ER chaperones is a critical process that contributes to efficient adipocyte differentiation. Thus, a physiological form of ER stress/UPR activation may be required for adipocyte differentiation in order to allow the cell to cope and adapt to an increased ER folding demand. Furthermore, mice with higher levels of ER stress have an increased rate of weight gain and obesity on a high-fat diet (10, 19). Hence, we tested the effect of 4-phenylbutyrate (4-PBA), a well-established chemical chaperone and inhibitor of ER stress, on adipogenesis and weight gain in a diet-induced obesity mouse model.

Many recent reports demonstrate that 4-PBA has chaperone properties and by stabilizing protein conformation in the ER, it can repress ER stress/UPR activation in vitro and in vivo (14, 19, 27–40). 4-PBA was found to restore glucose homeostasis, enhance insulin sensitivity, and decrease fatty liver disease in the diabetic *ob/ob* mouse model (14). More recent studies identified the ability of 4-PBA to enhance leptin sensitivity in vitro and in obese mice by decreasing ER stress-mediated leptin resistance (19). However, the effect of chemical chaperones, such as 4-PBA, on adipogenesis and diet-induced weight gain has not been investigated. In this study, murine 3T3-L1 cells were used to examine UPR activation during adipocyte differentiation. Our in vitro findings demonstrate that 4-PBA attenuates UPR activation that occurs during 3T3-L1 adipogenesis and prevents their differentiation. We also demonstrate that 4-PBA reduces the expression of the ER chaperone GRP78 in the adipose tissue of mice and decreases weight gain and fat mass, leading to decreased plasma glucose, triglycerides, adiponectin, and leptin levels in a diet-induced obesity mouse model. Importantly, these studies provide a solid foundation for the development of therapeutic approaches aimed at targeting the UPR to reduce the risk of obesity and its complications.

MATERIALS AND METHODS

Cell culture and adipocyte differentiation

3T3-L1 cells were purchased from ATCC and cultured in 5% CO₂ at 37°C. Cells were replaced in growth media consisting of DMEM (Invitrogen), 10% FBS (Invitrogen), 2 mM L-glutamine (Sigma), 50 units/ml penicillin, and 50 μ g/ml streptomycin (Sigma). For differentiation experiments, 3T3-L1 preadipocytes were allowed to reach confluence and cultured with stimulation/differentiation media consisting of growth media supplemented with MDI (0.5 mM 3-isobutyl-1-methyl-xanthine, 250 nM dexamethasone, and 10 μ g/ml insulin; Sigma). After 2 days in stimulation media, cells were placed in poststimulation media containing DMEM, 10% FBS, and 5 μ g/ml of insulin. Media were changed every 2 days until cells were lysed for Western blotting or fixed for Oil red O staining. *Xbp1*^{-/-} and wild-type mouse embryonic fibroblasts (MEFs) were a kind gift from Dr. Randal Kaufman (University of Michigan). Differentiation was induced using stimulation media with the addition of 5 μ M rosiglitazone (Cayman Chemicals) for the initial 48 h.

Treatment of cells with ER stress inhibitors. Cells were cultured in stimulation/differentiation media on day 0 and treated with 1–20 mM 4-PBA, 0.1–2 mg/ml of tauro-ursodeoxycholic acid, or 5–100 μ M salubrinal (Calbiochem). On day 2, media were changed to poststimulation media with readdition of the chemical chaperone unless otherwise specified.

Oil red O staining and lipid quantification

Staining of cells with Oil red O. Adherent cells were washed once with PBS and fixed with 3.7% formaldehyde. Oil red O solution, prepared as previously described by Kuri-Harcuch and Green (41), was added to the wells and incubated for 1 h at room temperature. The solution was removed and the plates were washed with distilled water. Images were taken using a Leica DM1L microscope equipped with a Canon PC1192 Powershot S31S camera.

Lipid quantification. The Oil red O stain was removed and quantified as described previously (42). Equal volumes of 60% isopropanol were added to the culture dishes to destain the fixed cells. The solution containing the Oil red O stain was collected, and absorbance was measured at 510 nm using a spectrophotometer (SpectraMAX Plus, SOFTmax Pro 4.0).

Metabolic protein labeling

To assess de novo protein synthesis, 3T3-L1 cells were grown to confluence (day 0) and washed with cysteine/methionine-free DMEM. Cells were then treated with 2 μ Ci/ml of L-[³⁵S]methionine (Perkin-Elmer) in cysteine/methionine-free and serum-free DMEM for 4 h at 37°C. The cells were washed and cultured in cysteine/methionine-free media overnight. The next day, the media were collected and frozen (for analysis of labeled secretory proteins), while total protein lysates were collected in SDS-lysis buffer for autoradiogram analysis of total labeled protein content. Experiments were repeated on days 2 and 7 of differentiation. Counts per minute were measured using a scintillation counter (Beckman LS 6000LL).

Cell lysis and protein isolation

Cells in culture dishes were washed twice with ice-cold PBS. SDS-lysis buffer (60 mM Tris-Cl, pH 6.8, 12.8% glycerol, and 2.05% SDS) containing protease inhibitors (Roche) was added to the cells. The cells were then scraped off and the lysates were frozen at –20°C.

Western blotting

Total protein concentration in each sample was measured using the Lowry protein assay kit (Bio-Rad). Equivalent amounts of protein lysates were separated on SDS-PAGE mini gels, transferred to nitrocellulose membranes, and incubated with primary antibodies for 2 h with gentle shaking at room temperature or overnight at 4°C. The following primary antibodies were used and diluted as per the manufacturer's recommendations: mouse anti-PPAR γ (Upstate), rabbit anti-calreticulin (Affinity Bioreagents), rabbit anti-phospho-eIF2 α , rabbit anti-GAPDH (Cell Signaling), mouse anti-KDEL, rabbit anti-protein disulfide isomerase (PDI), rabbit anti-NF κ B (Stressgen), mouse anti-GRP78 (BD Transduction), mouse anti-GADD153/C/EBP homologous protein (CHOP), rabbit anti-eIF2 α , rabbit anti-XBP-1 (Santa Cruz), rabbit anti-peroxiredoxin1 (Enzo Lifesciences), and mouse anti- β actin antibody (Sigma). The membranes were incubated for 1 h with either anti-mouse or anti-rabbit horseradish peroxidase IgG secondary antibodies (DAKO EnVision). Chemiluminescence detection using Western Lightning Chemiluminescence Reagent plus (Perkin Elmer) was performed. Membranes were

exposed to imaging film (Kodak Bioflex Econo Scientific) and developed using a Kodak X-OMAT 1000A Processor.

For Western blotting using mouse liver or epididymal adipose tissues, frozen tissue was directly homogenized in SDS lysis buffer containing protease inhibitors using a tissue homogenizer. The samples were then centrifuged for 10 min at 10,000 rpm, and the clear protein layer was carefully removed and used for Western blotting.

ELISA and cytometric bead array mouse inflammation assay

A mouse adiponectin ELISA kit (R & D Systems) was used to assay secreted adiponectin from cultured 3T3-L1 cells and in mouse plasma. Mouse insulin and leptin ELISA kits (Linco Research) were used to detect insulin and leptin in mouse plasma. Inflammatory markers were measured in mouse plasma using the Cytometric bead array mouse inflammation kit (BD Biosciences). Assays were performed as per the manufacturer's protocol. All samples were measured in triplicate.

Mouse studies

Seventeen, 5–6 week old female C57BL/6 mice (Charles River Laboratory) were housed in mouse cages and allowed to acclimatize for at least 1 week. A high-fat diet (21.2% fat by weight and 40% kcal from fat) was purchased from Harlan Teklad (88137). Pharmaceutical-grade 4-PBA sodium salt was purchased from Scandinavian Formulas. 4-PBA is soluble in water and thus was added to the drinking water fresh every week. At 10–11 weeks of age, all mice were fed ad libitum on the high-fat diet with or without 4-PBA supplementation for 120 days. Mice were fed a high-fat diet without (n = 8) or with (n = 9) 1g/kg/day of 4-PBA supplemented in the drinking water. Food and water intake measurements were made, and all of the mice were weighed at least once a week. Mice were anesthetized after 120 days using 4% isoflurane. Blood samples were collected for plasma glucose, cholesterol, and triglyceride measurements (Infinity Thermo Electron kit), as well as insulin, adiponectin, and leptin measurements using ELISA methods. Following cervical dislocation, epididymal fat pads and liver were collected for further study and analysis. None of the mice became ill or died as a result of the treatment. All procedures were approved by the McMaster University Animal Research Ethics Board.

Histology and adipocyte cell sizing

Liver and epididymal fat pads were fixed in formalin and paraffin embedded. Four micrometer sections of epididymal adipose tissue were deparaffinized and mounted unstained. Using 10 \times magnification, 5–10 representative images of each slide were captured and analyzed for cell size measurements (area in pixels) as described by Sauter et al. (43) using the computer imaging program ImagePro. For each group, 4–5 mice were included in the mean cell size and histogram analysis and a minimum of 500 cells were counted and sized. For morphological analysis of the liver sections, hematoxylin and eosin staining was performed, and representative images were obtained.

Mac-3 immunohistochemistry. Four micron thick sections were deparaffinized, and endogenous peroxidase activity was blocked with 0.5% H₂O₂ in methanol for 10 min. Sections were blocked with 5% normal rabbit serum, antigen heat-retrieved in citrate buffer at pH 6.0, and incubated with a rat anti-Mac-3 antibody (Pharming), diluted at 1:2,000. This was followed by a biotinylated rabbit anti-rat antibody, mouse adsorbed (Vector Laboratories) at a 1:500 dilution. Following streptavidin-peroxidase (Zymed), sections were developed in Nova Red peroxidase sub-

strate (Vector Laboratories) and counterstained with hematoxylin. Pictures were taken with a Laborlux S microscope (Leitz) equipped with an Olympus DP70 digital camera.

Hepatic triglyceride and cholesterol ester quantification

Frozen liver tissue (140 mg) was homogenized in a tissue grinder using buffer containing 10 mM HEPES, 20 mM MgCl₂, 10 mM β-mercaptoethanol, and 0.5% Triton X-100, at pH 7.0. Hexane/isopropanol (3:2, v/v) was added to each liver homogenate in glass tubes. The samples were spun down at 3,500 rpm for 3 min, and the organic layer was carefully removed. The hexane/isopropanol extraction was repeated three times, combining the organic phases in one tube. Following evaporation of the organic phase, triglyceride and cholesterol ester concentrations (mg/ml) were measured using the triglyceride assay kit (Infinity Thermo Electron) or Chol-E kit (Wako Diagnostics).

Statistical analyses

Statistical analyses were performed using Student's *t*-test assuming unequal variance and two-tailed distribution unless otherwise specified. Statistical significance was defined when $P < 0.05$. All results are presented as mean ± SD unless otherwise indicated.

RESULTS

Lipid accumulation and adiponectin secretion increase during adipocyte differentiation

3T3-L1 cells accumulate a significant amount of lipid droplets, as visualized by Oil red O staining, starting on day 4 of differentiation, gradually increasing their lipid content as they differentiate (Fig. 1A). Quantification of the Oil red O staining allowed for measurement of the extent of lipid accumulation as measured in Fig. 1B. Consistent with these findings, a significant and robust increase in the secretion of adiponectin (adipocytokine marker of differentiated cells) was observed in the culture media on days 4 and 7 of differentiation (Fig. 1C).

Markers of ER stress/UPR activation increase during adipocyte differentiation with increased de novo protein synthesis

To demonstrate that differentiating adipocytes are metabolically active, de novo protein synthesis was studied during 3T3-L1 differentiation. As seen in Fig. 2A, day 7 differentiated 3T3-L1 cells showed a significant increase in the secretion of ³⁵S-radiolabeled proteins into the culture media, as compared with preadipocytes. Consistent with these findings, autoradiogram of whole-cell lysates indicated an overall increase in the number and intensity of protein bands in day 7 cells (Fig. 2B), suggesting an increase in de novo protein synthesis following differentiation.

The expression of PPAR γ , the master regulator of adipogenesis, increased by day 5 of differentiation (Fig. 2C), consistent with the increase in adiponectin secretion and Oil red O staining. Markers of UPR activation, including the ER chaperones GRP78, PDI, and calreticulin (data not shown), as well as CHOP, phospho-eIF2 α , and spliced XBP1, were also differentially expressed during adipocyte differentiation (Fig. 2C). The increase in GRP78 levels observed in the later stages of differentiation coincides with the increased de novo protein synthesis in day 7 cells (Fig.

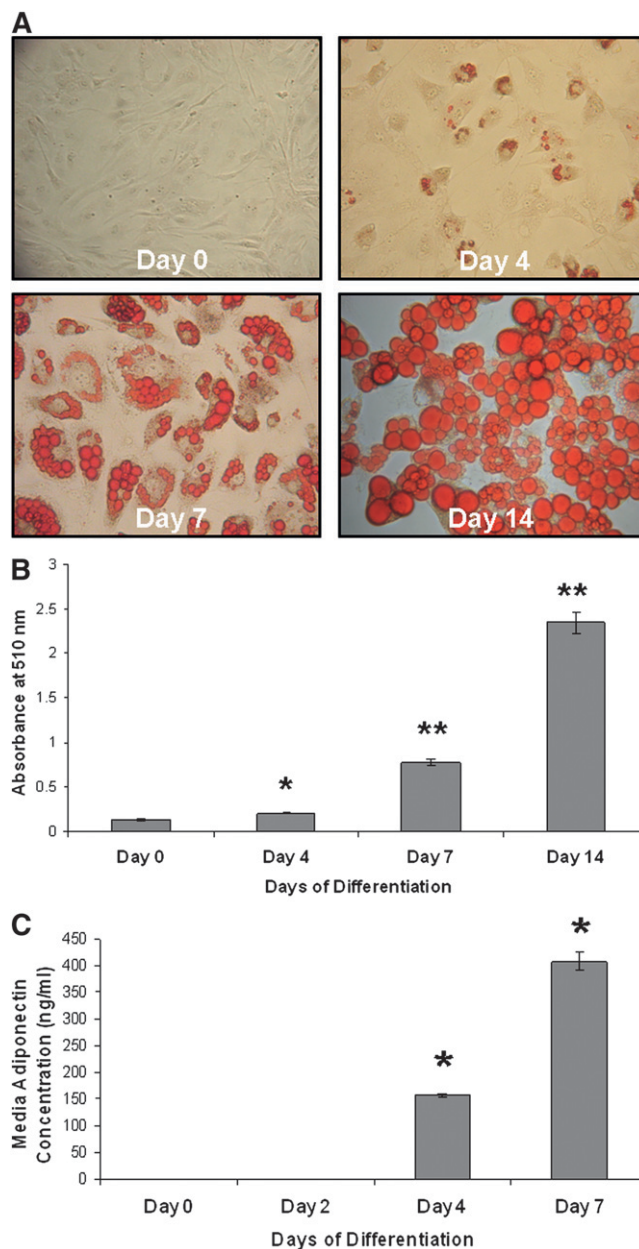


Fig. 1. Lipid accumulation and adiponectin secretion increase during adipocyte differentiation. A: Lipid accumulation increases with differentiation of 3T3-L1 cells. 3T3-L1 cells grown to confluence were differentiated in growth media containing MDI. Cells were washed in PBS, fixed with 3.7% formaldehyde, stained with Oil red O for 1 h, and photographed on day 0 (preadipocytes) and days 4, 7, and 14 of differentiation. B: Quantification of Oil red O staining in differentiating 3T3-L1 cells. Oil red O was extracted from the cells using 60% isopropanol and collected, and the absorbance was measured at 510 nm from cells on days 0, 4, 7, and 14 of differentiation ($*P < 0.0005$, $**P < 0.00001$ compared with day 0; $n = 3$). C: Adiponectin secretion from 3T3-L1 cells increases significantly following differentiation. 3T3-L1 cells were grown to confluence and cultured in differentiation media. Media were collected on days 0, 2, 4, and 7, and adiponectin levels were measured using ELISA. Concentrations in the samples were determined using a standard curve ($*P \leq 0.000001$ compared with day 0; $n = 3$).

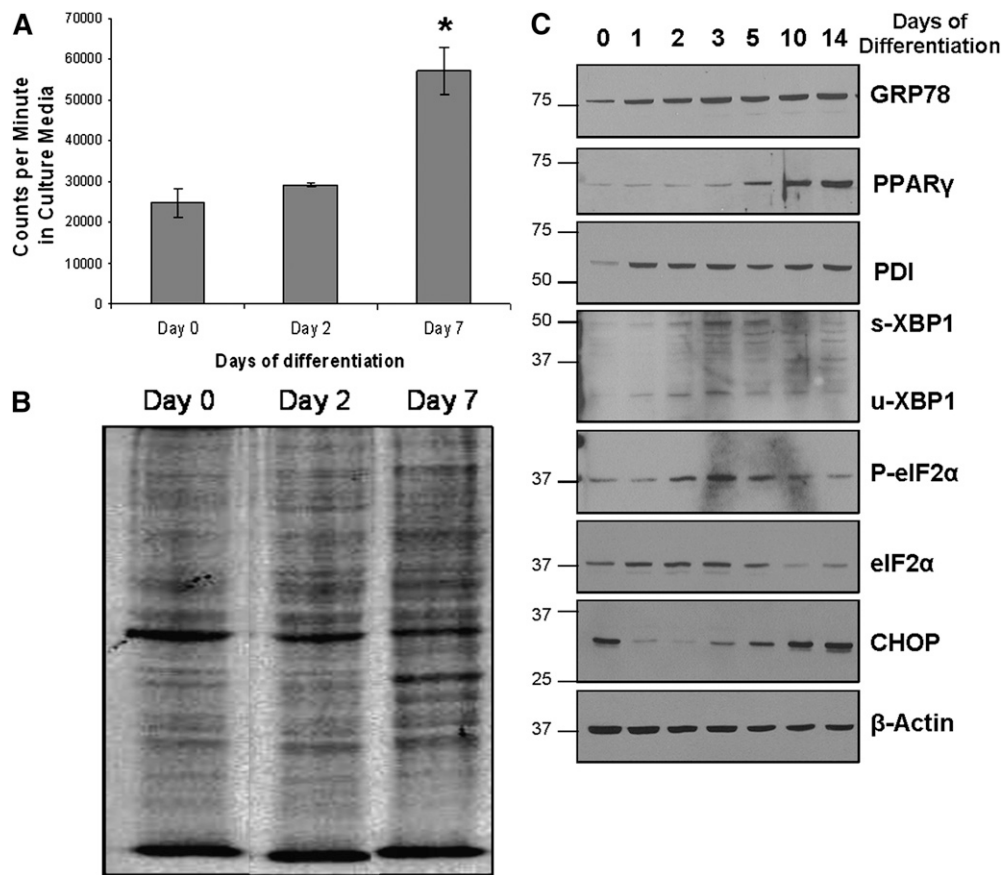


Fig. 2. UPR activation correlates with increased de novo protein synthesis during adipocyte differentiation. **A:** Differentiating 3T3-L1 cells display increased de novo protein synthesis and secretion. 3T3-L1 cells on days 0, 2, and 7 of differentiation were cultured for 4 h in cysteine/methionine-free media containing ^{35}S -methionine, washed, and incubated overnight in cysteine/methionine-free media. Media were collected the next day, and counts per minute of radioactivity were measured using a scintillation counter ($*P \leq 0.001$ compared with day 0; $n = 3$). **B:** Total protein lysates from the ^{35}S -labeling experiment were collected, and equivalent concentrations were loaded onto a 10% SDS polyacrylamide gel. The gel was subsequently dried and exposed to X-ray film for 48 h. The autoradiogram is shown here. **C:** Upregulation of ER stress/UPR markers occurs during 3T3-L1 differentiation. Cells were allowed to differentiate up to 14 days, and total protein lysates were collected in SDS lysis buffer at various time points. Protein was quantified using a Lowry protein assay, and equivalent amounts (30 μg) of protein were loaded into each well. Western blotting was performed to detect the following ER stress/UPR markers: GRP78, PDI, spliced and unspliced XBP1, phosphorylated and total eIF2 α , and CHOP. Blots were also probed for PPAR γ (marker of adipocyte differentiation) and β -actin to control for protein loading.

2A, B). Expression of spliced XBP-1 and phosphorylation of eIF2 α , which are downstream of the IRE-1 and PERK pathway, respectively, peaked around day 3, while CHOP followed a biphasic pattern of expression with increased levels in the later stages of differentiation.

The chemical chaperone 4-PBA inhibits adipogenesis and blocks UPR signaling

We sought to block ER stress/UPR signaling during adipogenesis to determine whether activation of the UPR pathways is required for adipocyte differentiation. Treatment of 3T3-L1 cells with the chemical chaperone and ER stress inhibitor 4-PBA on day 0 over a period of five days dose-dependently inhibited differentiation and lipid accumulation in 3T3-L1 cells as compared with untreated control cells (**Fig. 3A**). Similar dose-dependent inhibitory effects on differentiation were observed using another

well-documented chemical chaperone tauro-ursodeoxycholic acid (14, 34, 37) (see supplementary Fig. 1). Five days of 4-PBA treatment at doses of 10 or 20 mM significantly attenuated lipid accumulation, as measured by Oil red O staining in day 5 3T3-L1 cells (**Fig. 3B**). To confirm that adipogenesis was blocked in the presence of 4-PBA, adiponectin secretion into the media was measured, and a significant dose-dependent reduction in adiponectin concentration was observed in cells treated with 4-PBA, as compared with untreated day 5 cells (**Fig. 3C**). To exclude the possibility that the reduction in adipocyte differentiation and adiponectin secretion was due to cytotoxicity imposed by 4-PBA treatment, an LDH release/cytotoxicity assay was performed and the result confirmed that 48 h of 10 mM 4-PBA treatment was not toxic to 3T3-L1 cells (**Fig. 3D**). Additionally, 4-PBA itself did not interfere with the LDH release assay (data not shown).

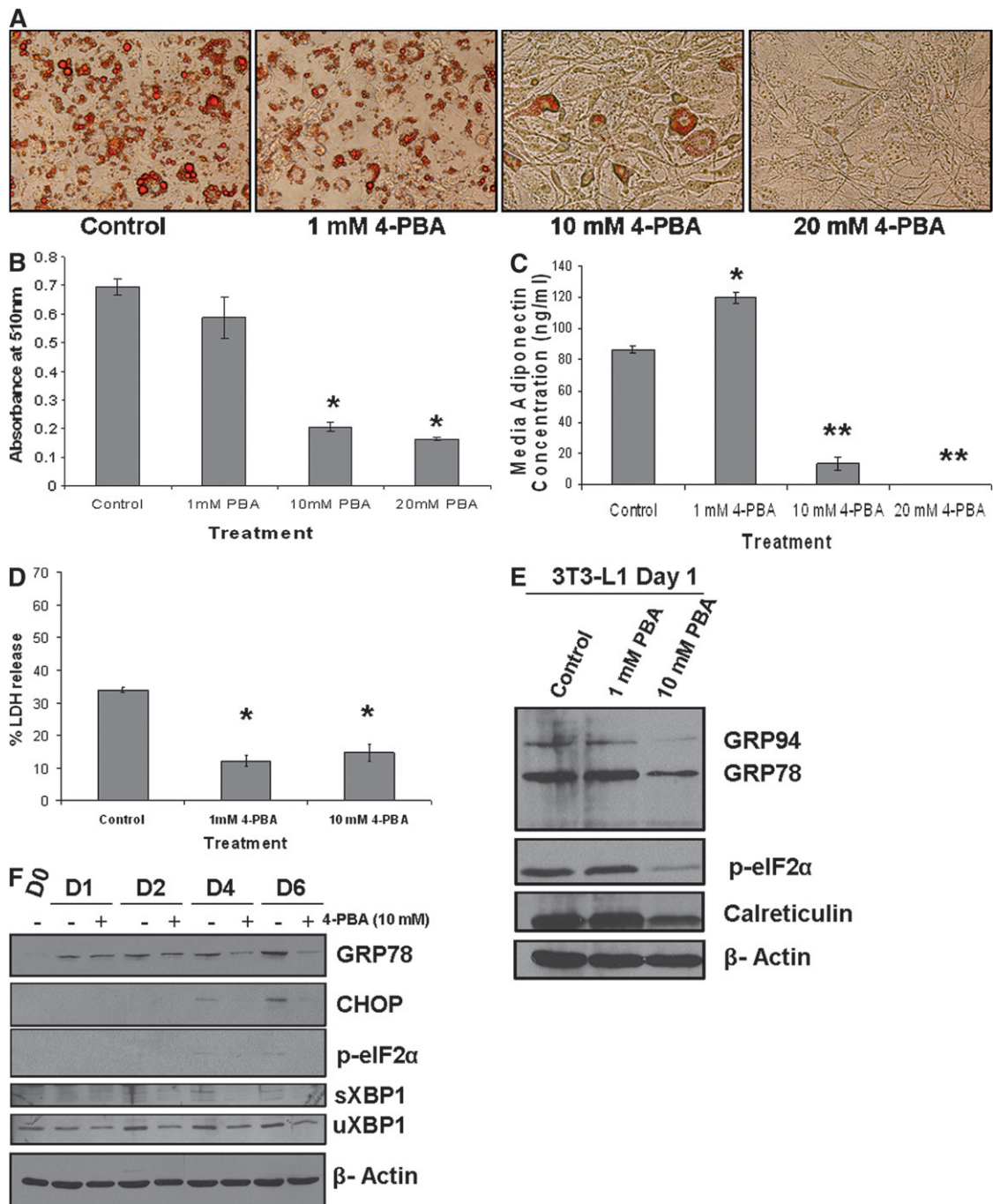


Fig. 3. Treatment of 3T3-L1 cells with 4-PBA inhibits UPR activation and blocks differentiation in a dose-dependent manner. **A:** Inhibition of Oil red O staining in differentiating 3T3-L1 cells by 4-PBA. Confluent 3T3-L1 cells were cultured in differentiation media with increasing concentrations of 4-PBA. On day 5, cells were fixed and stained with Oil red O. Representative images of Oil red O-stained cells are shown for each condition. **B:** Quantification of Oil red O indicates a significant decrease in lipid droplets with 4-PBA treatment. Following extraction and collection of Oil red O in isopropanol, absorbance was measured at 510 nm ($*P < 0.001$ compared with control; $n = 3$). **C:** Adiponectin secretion of 3T3-L1 cells is inhibited by 4-PBA. Media were collected on day 5 of differentiation, and adiponectin levels were measured using an ELISA ($*P \leq 0.0005$, $**P \leq 0.00001$ compared with control; $n = 3$). **D:** 4-PBA treatment is not cytotoxic to 3T3-L1 cells. Confluent 3T3-L1 cells were treated with 1 or 10 mM 4-PBA in 1% FBS media for up to 48 h. Media were collected, and LDH release was measured ($*P < 0.0005$; $n = 3$). **E:** Downregulation of UPR markers in 3T3-L1 cells following treatment with 4-PBA. Confluent 3T3-L1 cells were treated with 1 or 10 mM 4-PBA. After 24 h, total cell lysates were collected and run on a 10% SDS polyacrylamide gel. Antibodies against KDEL (to detect GRP78 and GRP94), calreticulin, phospho-eIF2 α , or β -actin were used for Western blotting. **F:** Differentiation of 3T3-L1 cells in the presence of 4-PBA suppresses GRP78 expression. 3T3-L1 cells were stimulated to differentiate in the presence or absence of 10 mM 4-PBA. Protein was collected on day 0 (confluent cells with no 4-PBA treatment) or days 1, 2, 4, and 6 of differentiation, and Western blotting was used to detect GRP78, CHOP, phospho-eIF2 α , and spliced XBP1. As a loading control, the membrane was probed for β -actin.

In order to assess the effects of 4-PBA on UPR activation in 3T3-L1 cells, Western blotting was performed on protein lysates from day 1 of differentiation with 4-PBA (24 h of treatment in differentiation media). The basal expression of GRP78, GRP94, phospho-eIF2 α , and calreticulin was reduced with 10 mM 4-PBA treatment (Fig. 3E). This confirmed that 4-PBA results in attenuation of UPR signaling and ER stress in 3T3-L1 cells over 24 h. Importantly, differentiation of 3T3-L1 cells in the presence of 10 mM 4-PBA not only blocked adipogenesis (Fig. 3A) but also inhibited the increase in GRP78, CHOP, p-eIF2 α , and spliced XBP1 expression that occurs during adipocyte differentiation (Fig. 3F). The reduction in GRP78 expression with 4-PBA treatment was more evident on day 6 of differentiation when 3T3-L1 cells have elevated levels of endogenous GRP78. Surprisingly, CHOP, an ER stress marker and negative regulator of adipogenesis, was induced in the first 24 h of 4-PBA treatment (data not shown). Knockdown of CHOP using small interference RNA was performed to determine whether upregulation of CHOP by 4-PBA is the underlying mechanism responsible for the inhibition in adipogenesis. Western blotting confirmed efficient knockdown of CHOP (see supplementary Fig. IIA); however, as shown in supplementary Fig. IIB and C, CHOP small interference RNA did not rescue the cells from the inhibitory effects of 4-PBA on adipogenesis. In addition, to rule out other factors that may be affected by 4-PBA that result in attenuation of adipogenesis, expression of NF κ B or β -catenin, which are known to inhibit adipogenesis (44–46), was assessed by Western blotting (see supplementary Fig. VA). No significant changes in the expression of these proteins was noted with 4-PBA over 48 h.

XBP1 deficiency decreases adipogenesis

MEFs deficient in PERK, one of the mediators of UPR signaling, have decreased lipogenic and adipogenic potential (24). Given that XBP1 gene expression and splicing have previously been shown to be important for lipogenesis in the liver (26) and since splicing of XBP1 increases during adipogenesis (Fig. 2C), we reasoned that deficiency of XBP1 would impair adipogenesis. To illustrate this, *Xbp1*^{-/-} MEFs were stimulated to differentiate for 4 days and compared with wild-type MEFs. Oil red O staining on days 0, 2, and 4 of differentiation clearly demonstrated a significant impairment in lipid accumulation in the *Xbp1*^{-/-} MEFs (Fig. 4A, B). Furthermore, treatment of 3T3-L1 cells with salubrinal, an inhibitor of ER stress that selectively inhibits eIF2 α dephosphorylation (47), dose-dependently inhibited adipocyte differentiation as measured by Oil red O staining (see supplementary Fig. IIIA). At the 100 μ M dose, salubrinal completely blocked lipid accumulation (see supplementary Fig. IIIA, B) and decreased XBP-1 splicing in differentiating day 4 3T3-L1 cells (see supplementary Fig. IIIC), further strengthening the importance of UPR signaling during adipogenesis.

The chemical chaperone 4-PBA blocks lipid accumulation during all stages of adipocyte differentiation

To illustrate that the inhibitory effects of 4-PBA on adipocyte differentiation are more pronounced when UPR

activation occurs (as shown in Fig. 2C, day 3 onwards), 3T3-L1 cells were treated with 10 mM 4-PBA during various stages of adipogenesis. As shown in Fig. 5A, cells that were treated with 4-PBA during the entire timeframe of the experiment (days 0–10) remained fibroblast-like with very little/undetectable lipid droplet formation. Adipocyte differentiation as measured by lipid accumulation was reduced regardless of when the cells were exposed to 4-PBA (Fig. 5A, B). Treatment with 4-PBA during days 0–2 with removal of the drug during days 2–10 allowed for some adipogenic conversion and lipid accumulation. Similarly, treatment with 4-PBA during the mid-stages of adipocyte differentiation (days 2–6) and its removal on day 6 allowed for further differentiation to occur between days 6 and 10. The reduction in Oil red O staining on day 10 of the experiment was significant with all of the different treatment conditions compared with control untreated day 10 cells (Fig. 5B). These findings demonstrate that the effect of 4-PBA is reversible once it is washed out and that the reduction in basal levels of UPR markers during early stages (days 0–2) can also impact on the rate of adipogenesis. However, when the initial 4-PBA treatment occurred from days 2–6 or 6–10, it had the most pronounced effect on lipid accumulation ($P < 0.05$ as compared with days 0–2 treatment). These data suggest that the inhibitory effect of 4-PBA is not specific to or dependent on any critical event during adipocyte differentiation but that its inhibitory effect on adipogenesis is related to the period of time when UPR activation occurs (about 3 days following the onset of differentiation).

Given that rosiglitazone, a potent PPAR γ agonist, can accelerate adipocyte differentiation, we investigated whether driving this process using rosiglitazone could override the effect of 4-PBA on adipocyte differentiation or vice versa. Supplementary Fig. IVA demonstrates that a combination of 10 mM 4-PBA and 4 μ M rosiglitazone treatment from days 0–5 of differentiation leads to a mixed cellular phenotype. The cells acquired the rounded phenotype similar to that of day 5 control or 4 μ M rosiglitazone treated cells; however, the extent of lipid accumulation was significantly reduced (see supplementary Fig. IVB). Rosiglitazone treatment alone increased the secretion of adiponectin compared with control day 5 cells as expected, but cotreatment with 4-PBA significantly reduced adiponectin secretion from 3T3-L1 cells. Importantly, adiponectin secretion from the co-treated cells was greater than the 4-PBA treated cells (see supplementary Fig. IVC). These results suggest that the presence of the PPAR γ -agonist rosiglitazone can partially rescue the inhibitory effect of 4-PBA on adipocyte differentiation. Western blotting results in supplementary Fig. IVD showed that 4-PBA-treated adipocytes at day 5 had blunted expression of GRP78 and GRP94. Rosiglitazone treatment, on the other hand, increased these chaperone levels compared with day 5 control protein lysates. However, rosiglitazone was not found to be an ER stress-inducing agent, as it did not upregulate GRP78/GRP94 levels (data not shown). The increase in GRP78 and GRP94 expression observed in differentiating day 5 cells is therefore most likely to be associated with accelerated adipogenesis

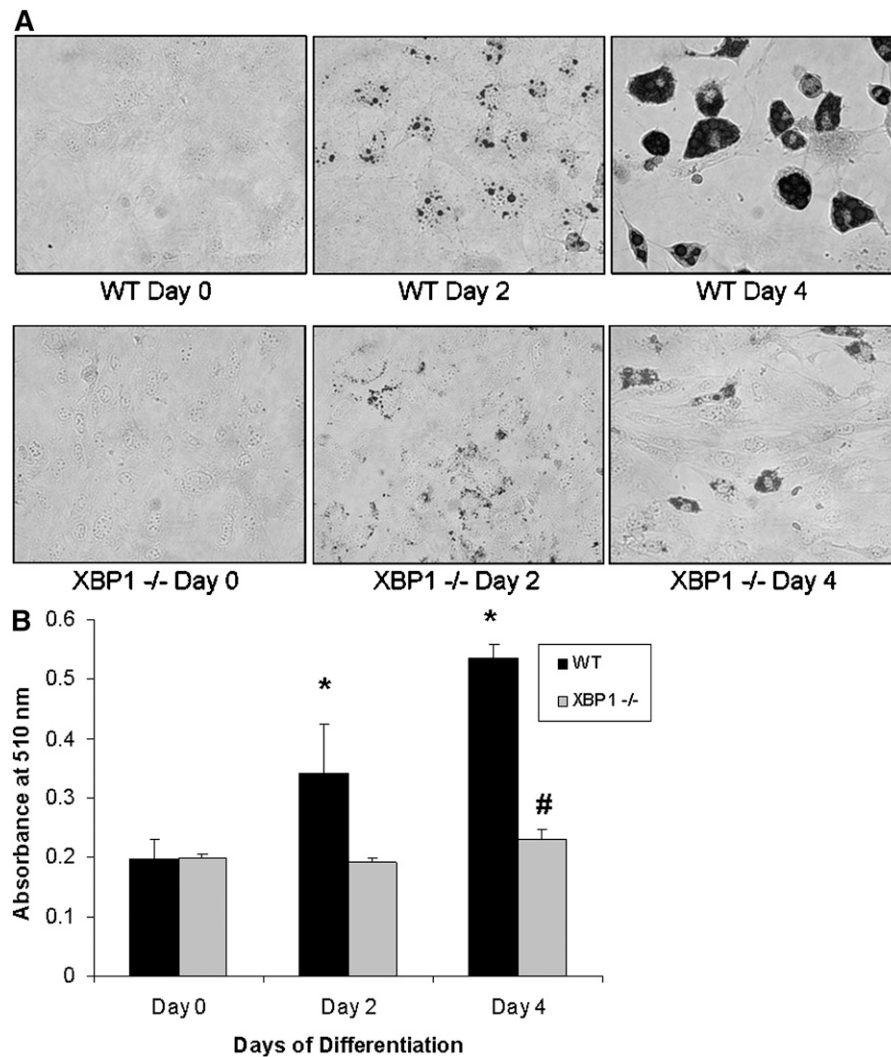


Fig. 4. XBP1-deficient MEFs have reduced adipogenic potential. A: *Xbp1*^{-/-} MEFs exhibit impaired adipogenesis. Wild-type (WT) or *Xbp1*^{-/-} MEFs were stimulated to differentiate into adipocytes for 4 days. Cells on days 0, 2, or 4 of differentiation were fixed and stained with Oil red O. B: Quantification of Oil red O staining. Wild-type MEFs accumulate lipid and demonstrate a significant increase in Oil red O staining, while deficiency of XBP1 prevents lipid accumulation (**P* < 0.01 compared with wild-type day 0 cells, #*P* < 0.05 compared with day 0 *Xbp1*^{-/-} MEFs; n = 6).

in day 5 cells exposed to rosiglitazone. Interestingly, co-treatment with rosiglitazone and 4-PBA partially reversed the suppression of chaperone levels observed with 4-PBA treatment alone and led to an increase in GRP78 expression in day 5 3T3-L1 cells (see supplementary Fig. IVD). Thus, the increased Oil red O staining and adiponectin secretion with rosiglitazone and 4-PBA co-treatment compared with 4-PBA treatment alone may possibly be due to increased UPR activation that is associated with enhanced adipocyte differentiation.

4-PBA supplementation of C57BL/6 mice fed a high-fat diet impairs weight gain and decreases epididymal fat mass and adipocyte size

To test the effect of 4-PBA on adipose tissue growth and weight gain in vivo, female C57BL/6 mice were fed a high-fat diet for 120 days supplemented with or without 1 g/kg/day of 4-PBA in the drinking water. As seen in Fig. 6A,

mice fed a high-fat diet supplemented with 4-PBA showed a significant resistance to weight gain starting at 63 days after commencing the experiment, while no difference in food intake was noted (Fig. 6B). The weight of the epididymal fat pads reflected the total weight of the animals (Fig. 6C), with the 4-PBA supplemented mice having significantly lower epididymal fat mass.

To examine the effect of 4-PBA on adipocyte differentiation and cell size, adipose tissues were fixed, paraffin embedded, and sectioned for fat cell sizing as described previously (48). Over 500 cells were sized for each mouse and at least four mice per group were included in the analysis. The histograms in Fig. 6D show the distribution of adipocyte cell sizes in the epididymal adipose tissue of mice supplemented with or without 4-PBA. The distribution was shifted to the left in the mice supplemented with 4-PBA, indicating an overall reduction in adipocyte size. Representative images of the cross section of the epididymal

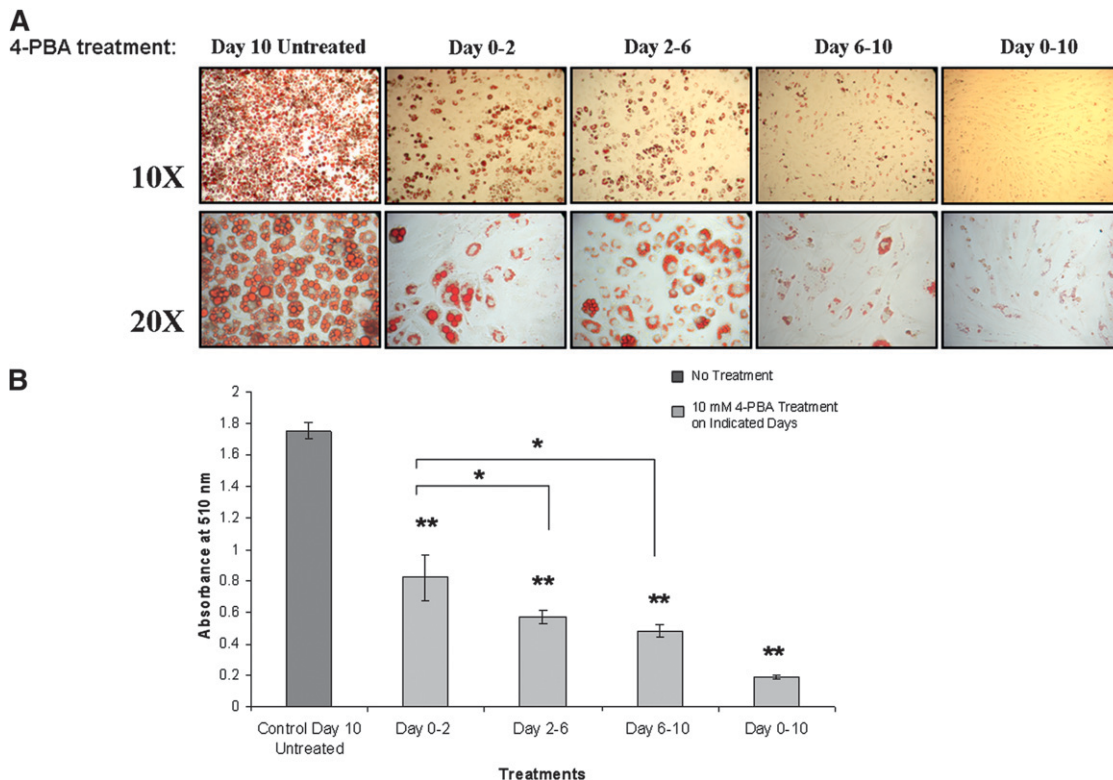


Fig. 5. 4-PBA inhibits lipid accumulation during all stages of differentiation. A: Effect of 4-PBA on Oil red O staining in differentiating 3T3-L1 cells. 3T3-L1 cells were treated with 10 mM 4-PBA at the onset of differentiation in the presence of MDI (days 0–2), during mid-stages after the MDI was removed (days 2–6), and during late stages after the majority of cells had differentiated (days 6–10). All cells were fixed and stained with Oil red O 10 days after commencing the experiment. As controls, cells were treated in the presence or absence of 4-PBA from days 0–10. B: Quantification of Oil red O staining in the absence or presence of 4-PBA at all stages of adipogenesis. Oil red O stain was quantified, and a significant reduction in lipid accumulation in all conditions was observed with 4-PBA treatment compared with day 10 untreated control (** $P < 0.001$; $n = 3$). The decline in lipid content was most dramatic in cells treated with 4-PBA during the later stages of adipogenesis: on days 2–6 or 6–10 ($*P < 0.05$ compared with days 0–2).

mal adipose tissue from the two groups of mice are shown in Fig. 6E. The mean cell size in the 4-PBA supplemented group was found to be significantly smaller as demonstrated graphically in Fig. 6F. Since the epididymal adipose tissue weights were lower and mean adipocyte size was found to be smaller in 4-PBA-supplemented mice, it suggests that 4-PBA is potentially inhibiting the recruitment and differentiation of preadipocytes as well as preventing the hypertrophy of preexisting adipocytes in vivo.

Plasma glucose, triglyceride, adiponectin, and leptin levels decreased in mice supplemented with 4-PBA

To assess whether 4-PBA had a general effect on metabolic parameters, blood was collected at the end of the study and total plasma glucose, triglycerides, and cholesterol were measured in the fed state (Table 1). Plasma glucose concentrations were significantly lower in the 4-PBA-supplemented mice. Mice fed a high-fat diet + 4-PBA also had a significant decrease in triglyceride levels. However, cholesterol concentrations did not change following 4-PBA treatment. Although no significant differences in plasma insulin levels were observed between the groups, both adiponectin and leptin levels were significantly lower in the 4-PBA-supplemented mice, proportional to the reduced fat pad mass (Table 2). To determine whether

4-PBA modulates pro-inflammatory cytokine expression, IL-12p70, TNF α , IFN γ , MCP-1, and IL-6 were measured in the plasma samples (Table 3). No significant differences in circulating cytokines were observed between the groups.

Mice supplemented with 4-PBA have decreased expression of GRP78 in the adipose but not liver tissue

Given our observations in vitro, we sought to determine whether 4-PBA decreased body weight by inhibiting ER stress signaling/UPR activation in the adipose tissue. Western blot analysis of total adipose tissue lysates indicated that mice fed a high-fat diet supplemented with 4-PBA had lower expression of the ER stress marker GRP78 (Fig. 7A). Protein band quantification in Fig. 7B demonstrated that mice supplemented with 4-PBA had significantly lower expression of GRP78 compared with the control group. In contrast to adipose tissue, GRP78 and calreticulin protein levels were unaffected in the livers of 4-PBA-treated versus untreated mice (Fig. 7D). Furthermore, as expected with a high-fat diet, histological analysis revealed the presence of fatty liver in all mice. However, no differences in liver morphology (Fig. 7E) or extent of triglyceride or cholesterol ester accumulation were found with 4-PBA supplementation in C57BL/6 mice (Fig. 7F).

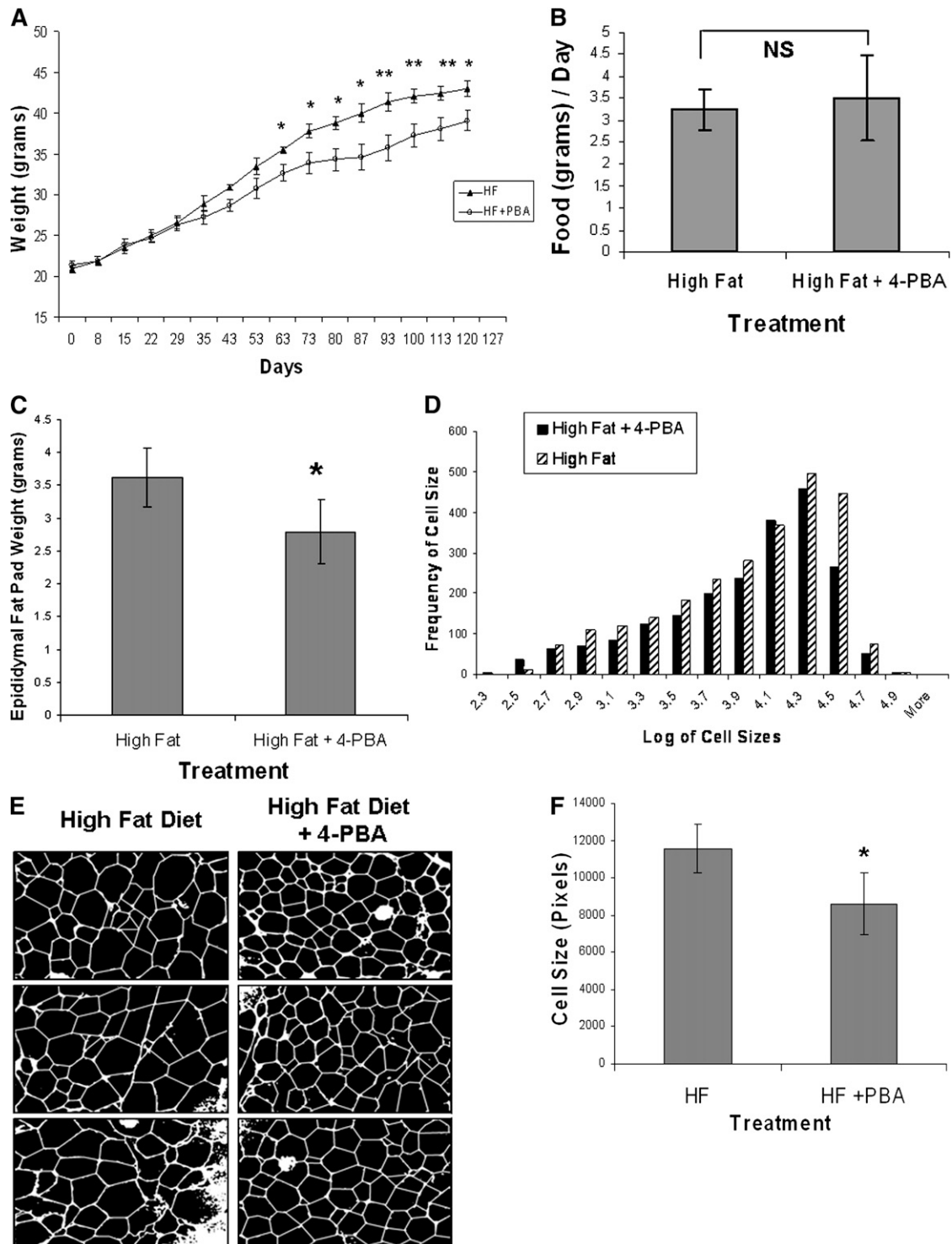


Fig. 6. Effect of 4-PBA on weight gain and adipogenesis in mice fed a high-fat diet. C57BL/6 mice were fed a high-fat diet supplemented without ($n = 8$) or with 4-PBA ($n = 9$) at a dose of 1g/kg/day. **A:** Effect of 4-PBA on weight gain. Starting at day 63 and for the remainder of the study, mice supplemented with 4-PBA had significantly lower body weights compared with controls ($*P \leq 0.05$, $**P \leq 0.01$ compared with the mice supplemented with 4-PBA using a rank sum test of significance; $n = 8-9$). **B:** Food intake measurements. No significant difference in food intake was noted between the two groups. **C:** Effect of 4-PBA on epididymal fat mass. Epididymal fat pads were removed at the conclusion of the study and weighed. Mice on the high fat + 4-PBA diet had significantly lower mean fat pad mass ($*P < 0.01$ using a rank sum test of significance; $n = 8-9$). **D:** Adipocyte cell size distribution from epididymal adipose tissue of C57BL/6 mice. The histograms represent the distribution of cell sizes in mice fed a high-fat diet with or without 4-PBA supplementation. The x axis represents the logarithm of cell sizes in pixels, while the y axis shows the frequency of a given cell size in the population of cells for each group of mice. **E:** Representative cross sections of epididymal fat pads. Images of the sectioned tissue were taken, and representative pictures from the two groups of mice are shown. **F:** Mean adipocyte size is reduced with 4-PBA supplementation. Mice fed a high-fat diet supplemented with 4-PBA had a significant reduction in average cell size compared with the high-fat diet alone group ($*P < 0.05$). For average cell size measurements, $n = 5$ for the high-fat group and $n = 4$ for the high-fat + 4-PBA group.

TABLE 1. Plasma concentrations of glucose, triglyceride, and cholesterol in high-fat diet fed mice supplemented with or without 4-PBA

	Glucose (mg/ml)	Triglyceride (mg/ml)	Cholesterol (mg/ml)
High fat	1.259 ± 0.183	0.555 ± 0.100	3.115 ± 0.241
High fat + 4-PBA	1.087 ± 0.067*	0.377 ± 0.096**	3.223 ± 0.389

Plasma was collected from C57BL/6 mice fed a high-fat diet with or without 4-PBA supplementation at 120 days. Nonfasting glucose (n = 7), triglyceride (n = 8), and cholesterol (n = 7) concentrations were determined as per the manufacturer's instructions. * $P \leq 0.05$ and ** $P \leq 0.005$ compared with 4-PBA nonsupplemented on the same diet.

Given that inflammation plays an important role in the pathogenesis of obesity (49–52), macrophage infiltration into the adipose tissue was assessed using immunohistochemical staining with a Mac-3 antibody. As shown in Fig. 7C, no differences in the extent of macrophage infiltration or crown-like structures were noted between the two groups of mice. Furthermore, Western blotting was performed to examine the effect of 4-PBA on inflammation or oxidative stress in 3T3-L1 cells as well as in the liver and adipose tissue lysates. As shown in supplementary Fig. VA, 4-PBA treatment of 3T3-L1 cells did not alter the expression of NFκB or peroxiredoxin-1, markers of inflammation and oxidative stress, respectively. Supplementation of mice with 4-PBA also did not alter the expression of NFκB or peroxiredoxin-1 in the adipose or liver tissues of mice (see supplementary Fig. VB).

DISCUSSION

Currently, there are two forms of UPR activation: acute and chronic/physiological. The acute form of the UPR occurs in response to adverse physiological conditions such as hypoxia, hyperglycemia, or viral infection that lead to ER stress. At the tissue level, nutrient excess, chronic inflammation, hypoxia, oxidative as well as mechanical stress due to adipocyte hypertrophy within the adipose tissue of obese individuals may lead to ER stress (11). This form of acute ER stress could adversely affect adipose function and contribute to type 2 diabetes, insulin resistance, leptin resistance, and lipotoxicity (10, 11, 19). The latter type of UPR activation occurs during cellular processes such as differentiation. This long-term physiological form of UPR activation likely takes place as a natural adaptive mechanism to ensure cell survival and efficient ER function dur-

TABLE 2. Plasma concentration of insulin, adiponectin, and leptin in high-fat diet-fed mice supplemented with or without 4-PBA

	Insulin (ng/ml)	Adiponectin (μg/ml)	Leptin (ng/ml)
High Fat	4.284±2.437	9.560±1.156	47.356±11.18
High Fat+4-PBA	6.099±2.196	8.200±0.827	35.873±3.893

Plasma was collected from C57BL/6 mice fed a high-fat diet with or without 4-PBA supplementation at 120 days. Insulin (n = 7), adiponectin (n = 6), and leptin (n = 7) concentrations were determined using ELISA kits. * $P \leq 0.05$.

ing cell processes such as differentiation of B cells into antibody producing plasma cells (53–55).

In this study, we report that a physiological form of UPR activation and the subsequent upregulation of ER chaperones occur during the process of adipogenesis. Expression of ER chaperones GRP78 and PDI increased during adipocyte differentiation. However, the expression of early markers of ER stress/UPR activation, such as phospho-eIF2α and spliced XBP1, peaked around day 3 and declined in the later stages of differentiation. Given that adipocytes synthesize and secrete large quantities of protein, it is likely that eIF2α is dephosphorylated in the late stages of adipogenesis to allow for efficient protein synthesis to occur since increased or prolonged phosphorylation of eIF2α would prevent the synthesis of proteins necessary for cellular differentiation and metabolic homeostasis (17, 56). In addition, the extent and duration of phosphorylated eIF2α and its downstream integrated stress response regulate PPARγ, C/EBPα, and β expression (17, 57, 58), which are pivotal transcription factors in adipogenesis. The transcription factor XBP1, on the other hand, is downstream of the IRE1 pathway and has been shown to be involved in hepatic lipogenesis (26). While there was an increase in spliced XBP1 during differentiation, it is unclear why the expression of both the spliced and unspliced forms of XBP1 decreased in the late stages of adipogenesis. In contrast, CHOP exhibited a biphasic pattern of expression, a finding consistent with a microarray analysis of 3T3-L1 cells (59). This finding is reasonable given that CHOP is a known negative regulator of adipogenesis (60), and early upregulation of CHOP following treatment with ER stress-inducing agents can block this process (61). While changes in the adipocyte during differentiation, such as alterations in the expression of specific transcription factors and kinases, may be modulating the UPR response, another potential underlying stimulus is the increased de novo protein synthesis and secretion that occurs in the mature adipocyte. Activation of the UPR primes the cell for the increased demand on the ER for proper folding and secretion of proteins. Therefore, an increase in ER chaperone expression would enable the cell to cope as it differentiates into a mature, metabolically active adipocyte. Since UPR activation occurs during adipocyte differentiation and adipogenesis is triggered during weight gain, mechanisms that relieve ER stress in the dysfunctional adipose tissue could be useful pharmacological strategies for preventing weight gain and obesity comorbidities. Thus, we explored the effect of an ER stress inhibitor, 4-PBA, on adipogenic conversion of 3T3-L1 cells and weight gain in a high-fat diet-induced obesity mouse model.

A number of studies have previously demonstrated that the low molecular weight fatty acid, 4-PBA, can act as a chemical chaperone, assisting with protein folding and thus relieving the cell of ER stress (14, 27–32, 62, 63). In this study, we demonstrated that 4-PBA can attenuate ER stress/UPR activation by decreasing the expression of GRP78, phospho-eIF2α, and spliced XBP1 in 3T3-L1 cells and attenuating adipogenesis. The observation that 4-PBA modulates lipid accumulation at any stage of the differen-

TABLE 3. Measurement of plasma pro-inflammatory markers in high-fat diet-fed mice supplemented with or without 4-PBA

	IL-12p70 (pg/ml)	TNF α (pg/ml)	IFN γ (pg/ml)	MCP-1 (pg/ml)	IL-6 (pg/ml)
High fat	9.69 \pm 3.23	6.41 \pm 0.67	2.17 \pm 0.49	61.05 \pm 24.66	2.44 \pm 0.71
High fat + 4-PBA	9.13 \pm 4.58	6.53 \pm 1.78	1.96 \pm 0.38	40.87 \pm 14.83	2.72 \pm 1.11

Plasma was collected from C57BL/6 mice fed a high-fat diet with or without 4-PBA supplementation at 120 days. Using bead flow cytometry, the concentration of each inflammatory marker was measured. IL-12p70 (n \geq 6), TNF α (n = 7); IFN γ (n = 7), MCP-1 (n \geq 6), IL-6 (n = 7). No significant differences were found.

tiation process, but more strikingly in the later stages, is important as it indicates that 4-PBA is not affecting the clonal expansion or preadipocyte growth arrest that occurs during the early stages of adipogenesis. Moreover, 4-PBA treatment at a stage when UPR activation occurs (day 2 onwards) had the most potent effect on lipid accumulation and adipocyte differentiation, confirming our hypothesis that 4-PBA likely blocks adipogenesis through attenuation of UPR signaling. Furthermore, co-treatment of 4-PBA with the PPAR γ agonist rosiglitazone drives the adipogenic pathway, and this alone results in enhanced UPR activation and GRP78 expression. Consequently, rosiglitazone can partially rescue the 4-PBA-mediated repression in adipogenesis.

It was surprising to find CHOP expression upregulated with 4-PBA in 3T3-L1 cells and loss-of-function studies revealed that upregulation of CHOP was not the mechanism by which 4-PBA inhibits adipogenesis in vitro. Additionally, CHOP was not upregulated in the adipose and liver tissues of 4-PBA-supplemented mice (data not shown). We explored the possibility that 4-PBA may be blocking adipogenesis through mechanisms unrelated to UPR signaling, such as changes in NF κ B or β -catenin, both of which have been shown to inhibit adipocyte differentiation (44–46). However, these proteins were unaffected by 4-PBA treatment. A well-documented mechanism of action of 4-PBA is its function as a histone deacetylase (HDAC) inhibitor (64, 65). It is therefore possible that its histone acetylase activity may be partially responsible for the inhibition of adipogenesis. However, recent findings on the effect of HDAC inhibitors on adipocyte differentiation are not conclusive. Most studies indicate that HDAC inhibitors stimulate adipocyte differentiation in 3T3-L1 cells (66–70), while one study suggests that inhibition of HDAC blocks adipogenesis (62). Because the overall findings of these studies imply that HDAC inhibitors act as stimulators of adipogenesis, and we found 4-PBA to have an inhibitory effect on differentiation, an HDAC-related mechanism of action can be excluded in this study. We suggest that reduced UPR signaling with 4-PBA through diminished splicing of XBP1 and/or decreased phosphorylation of eIF2 α play a significant role in its ability to block differentiation, as these genes are modulated during the normal course of adipogenesis and cells deficient in PERK or XBP1 exhibit impaired adipogenesis. Furthermore, decreased ER chaperone expression likely potentiates these effects as the cells become deficient in the ER folding machinery.

It is noteworthy that 4-PBA has other physiological functions in addition to its chaperone properties. It has been

clinically used to treat urea cycle disorders in children as well as sickle cell disease and thalassemia (27). 4-PBA was shown to be an efficient ammonia scavenger in C57BL/6 mice with hyperargininemia (71). Its function as an HDAC inhibitor and anticancer agent (64, 65, 72–74) as well as its potential as a therapeutic approach for the treatment of amyotrophic lateral sclerosis (28) have also been demonstrated. We chose to use the 10 mM dose of 4-PBA in vitro and 1 g/kg/day of 4-PBA in vivo, based on the study by Ozcan et al. demonstrating that 4-PBA can restore glucose homeostasis, improve insulin sensitivity, and resolve fatty liver disease in the *ob/ob* mice, a model of type 2 diabetes (14). In contrast to the study by Ozcan et al., high-fat diet-fed C57BL/6 mice supplemented with 4-PBA did not have lower plasma insulin levels or improved fatty liver disease, and these dissimilarities likely reflect differences in the strain and sex of the mice (male *ob/ob* versus female C57BL/6) and duration of the 4-PBA treatment (20 versus 120 days). Though Ozcan et al. did not find an effect of 4-PBA on body weight over the short duration of their study, we were interested to explore the ability of 4-PBA to affect diet-induced obesity over a much longer time frame. In addition, since 4-PBA is currently an orally administered drug (75–78), we tested its efficacy by dissolving it in the drinking water. Consistent with our in vitro findings, 4-PBA-supplemented mice had decreased GRP78 expression in the epididymal adipose tissue, indicating decreased ER stress/UPR activation. Interestingly, a recent report indicated that 4-PBA can decrease ER stress in the hypothalamus of obese mice and enhance leptin sensitivity (19). Therefore, this may represent an additional axis through which 4-PBA can be utilized as an anti-obesity treatment. Plasma leptin and adiponectin concentrations were measured in our study, and the decrease in these hormones was directly proportional to the adipose tissue mass, reflecting a decline in adipogenesis in vivo. The decrease in plasma glucose and triglyceride concentrations in the 4-PBA-supplemented mice was likely a reflection of the lower body mass and adipose tissue mass in this group. Taken together, these results confirm the in vitro finding that 4-PBA can attenuate ER stress and inhibit adipocyte differentiation/maturation, lipid accumulation, and adipocyte hypertrophy.

A combination of adipocyte hypertrophy and hyperplasia lead to an increase in adipose tissue mass and obesity. Our findings show that 4-PBA-supplemented mice on average had significantly smaller adipocytes and fat pad weight. We hypothesize that similar to our in vitro findings where 4-PBA treatment at various stages of adipogenesis affected

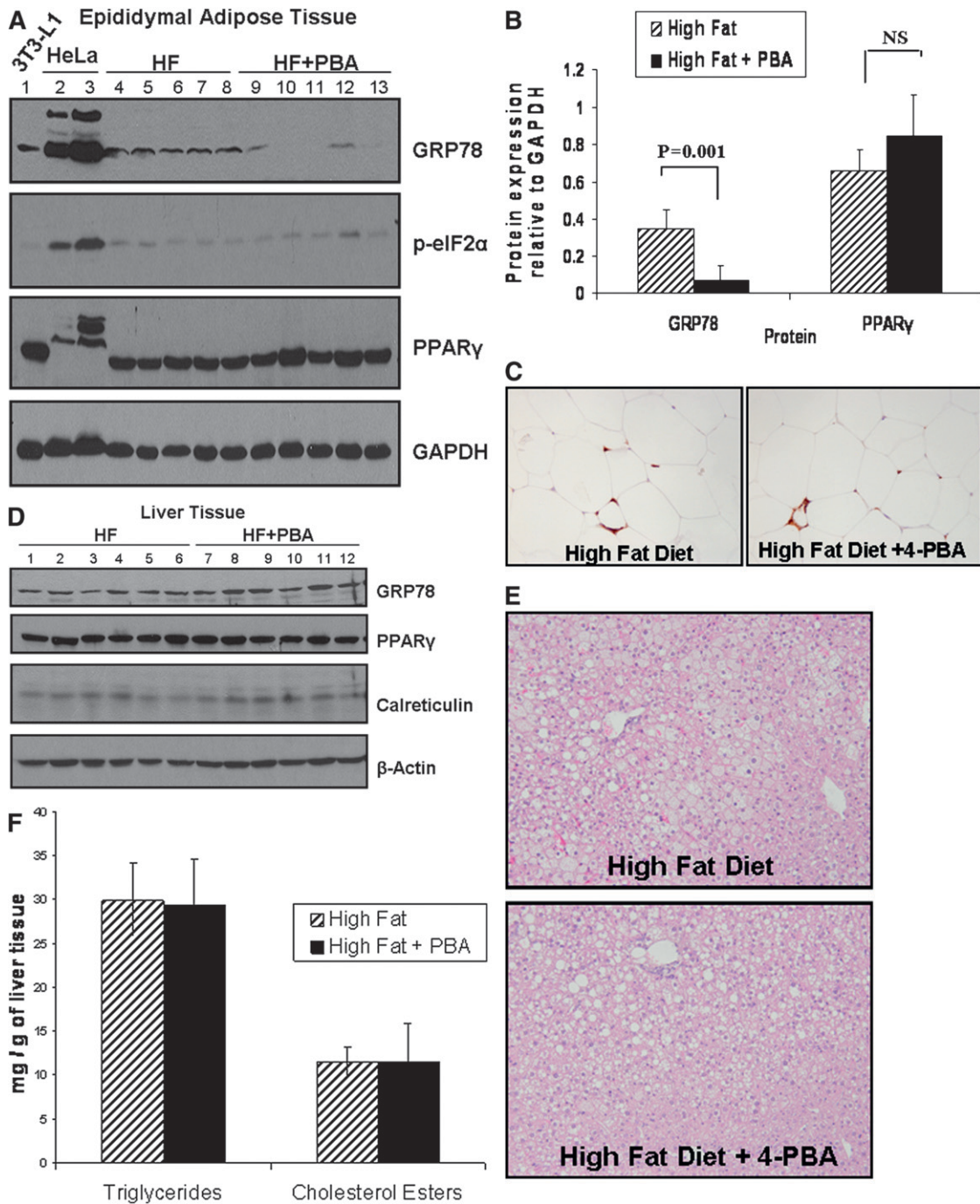



Fig. 7. 4-PBA treatment reduces GRP78 expression in the adipose but not liver tissue. **A:** Protein lysates from the epididymal adipose tissue of mice on high-fat diet (lanes 4–8) or high-fat diet + 4-PBA (lanes 9–13) were separated on a 10% SDS polyacrylamide gel. Membranes were probed for KDEL (to detect GRP78), PPAR γ , or phospho-eIF2 α . GAPDH was used as a loading control. Differentiated 3T3-L1 cell lysate (lane 1) and protein lysates from HeLa cells treated with the ER stress-inducing agent tunicamycin (lanes 2 and 3) were also loaded as positive controls for PPAR γ , GRP78, and phospho-eIF2 α expression, respectively. **B:** Band intensity quantification analysis demonstrated a significant decrease in GRP78 in the adipose tissues of 4-PBA-treated mice ($*P = 0.001$; $n = 5$). No significant difference was seen in PPAR γ or phospho-eIF2 α expression between the two groups of mice. **C:** Mac-3 staining of the adipose tissue. The epididymal adipose tissue was stained with an antibody against Mac-3 to detect infiltrated macrophages. Representative images are shown. **D:** Total liver lysates from mice on high-fat diet (lanes 1–6) or high-fat diet + 4-PBA (lanes 7–12) were separated on a 10% SDS polyacrylamide gel. Western blot analysis was used to detect the ER stress markers GRP78 and calreticulin, as well as PPAR γ and β -actin. No significant differences were seen between the two groups. **E:** Detection of fatty liver in mice fed high-fat diet or high-fat diet + 4-PBA. Fixed and paraffin-embedded liver samples were sectioned, deparaffinized, and stained with hematoxylin and eosin. Representative images from each group showed similar degrees of hepatic steatosis. **F:** Quantification of hepatic triglycerides and cholesterol esters. Approximately 150 mg of frozen liver tissue was homogenized, and triglycerides and cholesterol esters were extracted. No differences in triglyceride or cholesterol ester concentrations were observed between the two groups of mice ($n = 4$).

lipid storage and adipogenesis, 4-PBA *in vivo* is likely not only affecting adipocyte differentiation, but also playing a role in the maintenance of adipocytes at various sizes and stages of maturation. Therefore, it is possible that 4-PBA is directly affecting the dynamics of adipose tissue remodeling during the high-fat diet feeding. In contrast to the adipose tissue, we found no differences in plasma inflammatory cytokines or liver morphology, liver ER stress markers, or extent of fatty liver disease in the two groups of mice. Importantly, since adipose mass was reduced with 4-PBA and hepatic TG and cholesterol esters were not affected, it suggests that the lower plasma TG concentration in these mice is not due to enhanced storage in the liver or adipose tissue. A likely explanation is that 4-PBA has lipolytic properties that may inhibit TG formation or enhance its breakdown by rapid lipolysis or β -oxidation in the adipose or liver tissue. Alternatively, decreased UPR activation in the adipose tissue may inhibit the activation of sterol-regulatory element binding protein (SREBP-1) and/or -2, proteins involved in *de novo* lipid biosynthesis (79, 80). Therefore, an SREBP-mediated mechanism of action can also be a potential pathway to investigate since inhibition of ER stress by GRP78 overexpression decreases SREBP activation and reduces hepatic steatosis in mice (81).

In summary, we have demonstrated that UPR activation contributes to adipocyte differentiation and hypertrophy. Through the use of the chemical chaperone 4-PBA, we demonstrated that blocking UPR signaling can prevent adipocyte differentiation in 3T3-L1 cells and in the adipose tissue of high-fat diet-fed C57BL/6 mice. Further research into the role of 4-PBA on other cellular pathways and processes may shed more light on its potential as an anti-obesity and anti-diabetic drug. Based on our findings, a better understanding of the relation between UPR activation and adipogenesis *in vivo* would enhance the discovery of unique pharmacological and therapeutic approaches aimed at reducing the risk of obesity and its complications.

Note added in proof

Additional data in support of Fig. 4 has been added as supplementary Fig. VI, demonstrating that XBPI-deficient MEFs show reduced PPAR γ and C/EBP α protein expression upon stimulation with adipogenic media. These findings reinforce the results in Fig. 4, indicating reduced lipid accumulation in the XBPI-deficient MEFs following differentiation compared with wild-type MEFs. 

The authors thank Dr. Randal Kaufman for generously providing us with the *Xbp1*^{-/-} and wild-type MEFs. We thank Sue Beaudin for her assistance with the bead flow cytometry, Bilal Ahmed and Dr. Sudesh Sood for their technical assistance, Dr. Mahmood Akhtar for his helpful input and stimulating discussions, and Dr. Jeffrey Dickhout for his insightful comments on the manuscript.

REFERENCES

- Bray, G. A. 2004. Medical consequences of obesity. *J. Clin. Endocrinol. Metab.* **89**: 2583–2589.
- Kosti, R. I., and D. B. Panagiotakos. 2006. The epidemic of obesity in children and adolescents in the world. *Cent. Eur. J. Public Health.* **14**: 151–159.
- Gregoire, F. M., C. M. Smas, and H. S. Sul. 1998. Understanding adipocyte differentiation. *Physiol. Rev.* **78**: 783–809.
- Erol, A. 2005. Adipocyte insensitivity syndromes—novel approach to nutritional metabolic problems including obesity and obesity related disorders. *Med. Hypotheses.* **64**: 826–832.
- de Ferranti, S., and D. Mozaffarian. 2008. The perfect storm: obesity, adipocyte dysfunction, and metabolic consequences. *Clin. Chem.* **54**: 945–955.
- Green, H., and O. Kehinde. 1975. An established preadipose cell line and its differentiation in culture. II. Factors affecting the adipose conversion. *Cell.* **5**: 19–27.
- Kim, S., and N. Moustaid-Moussa. 2000. Secretory, endocrine and autocrine/paracrine function of the adipocyte. *J. Nutr.* **130**: 3110S–3115S.
- Kim, P. S., and P. Arvan. 1998. Endocrinopathies in the family of endoplasmic reticulum (ER) storage diseases: disorders of protein trafficking and the role of ER molecular chaperones. *Endocr. Rev.* **19**: 173–202.
- Schroder, M., and R. J. Kaufman. 2005. The mammalian unfolded protein response. *Annu. Rev. Biochem.* **74**: 739–789.
- Ozcan, U., Q. Cao, E. Yilmaz, A. H. Lee, N. N. Iwakoshi, E. Ozdelen, G. Tuncman, C. Gorgun, L. H. Glimcher, and G. S. Hotamisligil. 2004. Endoplasmic reticulum stress links obesity, insulin action, and type 2 diabetes. *Science.* **306**: 457–461.
- Gregor, M. F., and G. S. Hotamisligil. 2007. Thematic review series: Adipocyte Biology. Adipocyte stress: the endoplasmic reticulum and metabolic disease. *J. Lipid Res.* **48**: 1905–1914.
- Shen, X., K. Zhang, and R. J. Kaufman. 2004. The unfolded protein response—a stress signaling pathway of the endoplasmic reticulum. *J. Chem. Neuroanat.* **28**: 79–92.
- Hendershot, L. M. 2004. The ER function BiP is a master regulator of ER function. *Mt. Sinai J. Med.* **71**: 289–297.
- Ozcan, U., E. Yilmaz, L. Ozcan, M. Furuhashi, E. Vaillancourt, R. O. Smith, C. Z. Gorgun, and G. S. Hotamisligil. 2006. Chemical chaperones reduce ER stress and restore glucose homeostasis in a mouse model of type 2 diabetes. *Science.* **313**: 1137–1140.
- Ozawa, K., M. Miyazaki, M. Matsuhisa, K. Takano, Y. Nakatani, M. Hatazaki, T. Tamatani, K. Yamagata, J. Miyagawa, Y. Kitao, et al. 2005. The endoplasmic reticulum chaperone improves insulin resistance in type 2 diabetes. *Diabetes.* **54**: 657–663.
- Sreejayan, N., F. Dong, M. R. Kandadi, X. Yang, and J. Ren. 2008. Chromium alleviates glucose intolerance, insulin resistance, and hepatic ER stress in obese mice. *Obesity (Silver Spring). MD.* **16**: 1331–1337.
- Oyadomari, S., H. P. Harding, Y. Zhang, M. Oyadomari, and D. Ron. 2008. Dephosphorylation of translation initiation factor 2 α enhances glucose tolerance and attenuates hepatosteatosis in mice. *Cell Metab.* **7**: 520–532.
- Hosogai, N., A. Fukuhara, K. Oshima, Y. Miyata, S. Tanaka, K. Segawa, S. Furukawa, Y. Tochino, R. Komuro, M. Matsuda, et al. 2007. Adipose tissue hypoxia in obesity and its impact on adipocytokine dysregulation. *Diabetes.* **56**: 901–911.
- Ozcan, L., A. S. Ergin, A. Lu, J. Chung, S. Sarkar, D. Nie, M. G. Myers, Jr., and U. Ozcan. 2009. Endoplasmic reticulum stress plays a central role in development of leptin resistance. *Cell Metab.* **9**: 35–51.
- Boden, G., X. Duan, C. Homko, E. J. Molina, W. Song, O. Perez, P. Cheung, and S. Merali. 2008. Increase in endoplasmic reticulum stress-related proteins and genes in adipose tissue of obese, insulin-resistant individuals. *Diabetes.* **57**: 2468–2444.
- Sharma, N. K., S. K. Das, A. K. Mondal, O. G. Hackney, W. S. Chu, P. A. Kern, N. Rasouli, H. J. Spencer, A. Yao-Borengasser, and S. C. Elbein. 2008. Endoplasmic reticulum stress markers are associated with obesity in nondiabetic subjects. *J. Clin. Endocrinol. Metab.* **93**: 4532–4541.
- Gregor, M. F., L. Yang, E. Fabbrini, B. S. Mohammed, J. C. Eagon, G. S. Hotamisligil, and S. Klein. 2009. Endoplasmic reticulum stress is reduced in tissues of obese subjects after weight loss. *Diabetes.* **58**: 693–700.
- Rutkowski, D. T., J. Wu, S. H. Back, M. U. Callaghan, S. P. Ferris, J. Iqbal, R. Clark, H. Miao, J. R. Hassler, J. Fornek, et al. 2008. UPR pathways combine to prevent hepatic steatosis caused by ER stress-mediated suppression of transcriptional master regulators. *Dev. Cell.* **15**: 829–840.

24. Bobrovnikova-Marjon, E., G. Hatzivassiliou, C. Grigoriadou, M. Romero, D. R. Cavener, C. B. Thompson, and J. A. Diehl. 2008. PERK-dependent regulation of lipogenesis during mouse mammary gland development and adipocyte differentiation. *Proc. Natl. Acad. Sci. USA*. **105**: 16314–16319.
25. Yoshida, H., T. Matsui, A. Yamamoto, T. Okada, and K. Mori. 2001. XBP1 mRNA is induced by ATF6 and spliced by IRE1 in response to ER stress to produce a highly active transcription factor. *Cell*. **107**: 881–891.
26. Lee, A. H., E. F. Scapa, D. E. Cohen, and L. H. Glimcher. 2008. Regulation of hepatic lipogenesis by the transcription factor XBP1. *Science*. **320**: 1492–1496.
27. Qi, X., T. Hosoi, Y. Okuma, M. Kaneko, and Y. Nomura. 2004. Sodium 4-phenylbutyrate protects against cerebral ischemic injury. *Mol. Pharmacol.* **66**: 899–908.
28. Ryu, H., K. Smith, S. I. Camelo, I. Carreras, J. Lee, A. H. Iglesias, F. Dangond, K. A. Cormier, M. E. Cudkovic, R. H. Brown, Jr., et al. 2005. Sodium phenylbutyrate prolongs survival and regulates expression of anti-apoptotic genes in transgenic amyotrophic lateral sclerosis mice. *J. Neurochem.* **93**: 1087–1098.
29. Inden, M., Y. Kitamura, H. Takeuchi, T. Yanagida, K. Takata, Y. Kobayashi, T. Taniguchi, K. Yoshimoto, M. Kaneko, Y. Okuma, et al. 2007. Neurodegeneration of mouse nigrostriatal dopaminergic system induced by repeated oral administration of rotenone is prevented by 4-phenylbutyrate, a chemical chaperone. *J. Neurochem.* **101**: 1491–1504.
30. Kubota, K., Y. Niinuma, M. Kaneko, Y. Okuma, M. Sugai, T. Omura, M. Uesugi, T. Uehara, T. Hosoi, and Y. Nomura. 2006. Suppressive effects of 4-phenylbutyrate on the aggregation of Pacl receptors and endoplasmic reticulum stress. *J. Neurochem.* **97**: 1259–1268.
31. Lim, M., K. McKenzie, A. D. Floyd, E. Kwon, and P. L. Zeitlin. 2004. Modulation of deltaF508 cystic fibrosis transmembrane regulator trafficking and function with 4-phenylbutyrate and flavonoids. *Am. J. Respir. Cell Mol. Biol.* **31**: 351–357.
32. Vilatoba, M., C. Eckstein, G. Bilbao, C. A. Smyth, S. Jenkins, J. A. Thompson, D. E. Eckhoff, and J. L. Contreras. 2005. Sodium 4-phenylbutyrate protects against liver ischemia reperfusion injury by inhibition of endoplasmic reticulum-stress mediated apoptosis. *Surgery*. **138**: 342–351.
33. Mulhern, M. L., C. J. Madson, P. F. Kador, J. Randazzo, and T. Shinohara. 2007. Cellular osmolytes reduce lens epithelial cell death and alleviate cataract formation in galactosemic rats. *Mol. Vis.* **13**: 1397–1405.
34. de Almeida, S. F., G. Picarote, J. V. Fleming, M. Carmo-Fonseca, J. E. Azevedo, and M. de Sousa. 2007. Chemical chaperones reduce endoplasmic reticulum stress and prevent mutant HFE aggregate formation. *J. Biol. Chem.* **282**: 27905–27912.
35. Datta, R., A. Waheed, G. N. Shah, and W. S. Sly. 2007. Signal sequence mutation in autosomal dominant form of hypoparathyroidism induces apoptosis that is corrected by a chemical chaperone. *Proc. Natl. Acad. Sci. USA*. **104**: 19989–19994.
36. Sawada, N., J. Yao, N. Hiramatsu, K. Hayakawa, I. Araki, M. Takeda, and M. Kitamura. 2008. Involvement of hypoxia-triggered endoplasmic reticulum stress in outlet obstruction-induced apoptosis in the urinary bladder. *Lab. Invest.* **88**: 553–563.
37. Watanabe, N., and E. Lam. 2008. BAX inhibitor-1 modulates endoplasmic reticulum stress-mediated programmed cell death in Arabidopsis. *J. Biol. Chem.* **283**: 3200–3210.
38. Choi, S. E., Y. J. Lee, H. J. Jang, K. W. Lee, Y. S. Kim, H. S. Jun, S. S. Kang, J. Chun, and Y. Kang. 2008. A chemical chaperone 4-PBA ameliorates palmitate-induced inhibition of glucose-stimulated insulin secretion (GSIS). *Arch. Biochem. Biophys.* **475**: 109–114.
39. Haberzettl, P., E. Vladykovskaya, S. Srivastava, and A. Bhatnagar. 2009. Role of endoplasmic reticulum stress in acrolein-induced endothelial activation. *Toxicol. Appl. Pharmacol.* **234**: 14–24.
40. Hosoi, T., M. Sasaki, T. Miyahara, C. Hashimoto, S. Matsuo, M. Yoshii, and K. Ozawa. 2008. Endoplasmic reticulum stress induces leptin resistance. *Mol. Pharmacol.* **74**: 1610–1619.
41. Kuri-Harcuch, W., and H. Green. 1978. Adipose conversion of 3T3 cells depends on a serum factor. *Proc. Natl. Acad. Sci. USA*. **75**: 6107–6109.
42. Kasturi, R., and V. C. Joshi. 1982. Hormonal regulation of stearoyl coenzyme A desaturase activity and lipogenesis during adipose conversion of 3T3-L1 cells. *J. Biol. Chem.* **257**: 12224–12230.
43. Sauter, N. S., F. T. Schulthess, R. Galasso, L. W. Castellani, and K. Maedler. 2008. The anti-inflammatory cytokine IL-1Ra protects from high fat diet-induced hyperglycemia. *Endocrinology*. **149**: 2208–2218.
44. Suzawa, M., I. Takada, J. Yanagisawa, F. Ohtake, S. Ogawa, T. Yamauchi, T. Kadowaki, Y. Takeuchi, H. Shibuya, Y. Gotoh, et al. 2003. Cytokines suppress adipogenesis and PPAR-gamma function through the TAK1/TAB1/NIK cascade. *Nat. Cell Biol.* **5**: 224–230.
45. Chae, G. N., and S. J. Kwak. 2003. NF-kappaB is involved in the TNF-alpha induced inhibition of the differentiation of 3T3-L1 cells by reducing PPARgamma expression. *Exp. Mol. Med.* **35**: 431–437.
46. Prestwich, T. C., and O. A. Macdougald. 2007. Wnt/beta-catenin signaling in adipogenesis and metabolism. *Curr. Opin. Cell Biol.* **19**: 612–617.
47. Boyce, M., K. F. Bryant, C. Jousse, K. Long, H. P. Harding, D. Scheuner, R. J. Kaufman, D. Ma, D. M. Coen, D. Ron, et al. 2005. A selective inhibitor of eIF2alpha dephosphorylation protects cells from ER stress. *Science*. **307**: 935–939.
48. Sauter, N. S., F. T. Schulthess, R. Galasso, L. W. Castellani, and K. Maedler. 2008. The anti-inflammatory cytokine interleukin-1 receptor antagonist protects from high-fat diet-induced hyperglycemia. *Endocrinology*. **149**: 2208–2218.
49. Murano, I., G. Barbatelli, V. Parisani, C. Latini, G. Muzzonigro, M. Castellucci, and S. Cinti. 2008. Dead adipocytes, detected as crown-like structures, are prevalent in visceral fat depots of genetically obese mice. *J. Lipid Res.* **49**: 1562–1568.
50. Subramanian, V., and A. W. Ferrante Jr. 2009. Obesity, inflammation, and macrophages. *Nestle Nutr. Workshop Ser. Pediatr. Program*. **63**: 151–162.
51. Tordjman, J., M. Guerre-Millo, and K. Clement. 2008. Adipose tissue inflammation and liver pathology in human obesity. *Diabetes Metab.* **34**: 658–663.
52. Vachharajani, V., and D. N. Granger. 2009. Adipose tissue: a motor for the inflammation associated with obesity. *IUBMB Life*. **61**: 424–430.
53. Iwakoshi, N. N., A. H. Lee, and L. H. Glimcher. 2003. The X-box binding protein-1 transcription factor is required for plasma cell differentiation and the unfolded protein response. *Immunol. Rev.* **194**: 29–38.
54. Iwakoshi, N. N., A. H. Lee, P. Vallabhajosyula, K. L. Otipoby, K. Rajewsky, and L. H. Glimcher. 2003. Plasma cell differentiation and the unfolded protein response intersect at the transcription factor XBP-1. *Nat. Immunol.* **4**: 321–329.
55. Reimold, A. M., N. N. Iwakoshi, J. Manis, P. Vallabhajosyula, E. Szomolanyi-Tsuda, E. M. Gravallese, D. Friend, M. J. Grusby, F. Alt, and L. H. Glimcher. 2001. Plasma cell differentiation requires the transcription factor XBP-1. *Nature*. **412**: 300–307.
56. Marciniak, S. J., and D. Ron. 2006. Endoplasmic reticulum stress signaling in disease. *Physiol. Rev.* **86**: 1133–1149.
57. Calkhoven, C. F., C. Muller, and A. Leutz. 2002. Translational control of gene expression and disease. *Trends Mol. Med.* **8**: 577–583.
58. Dagon, Y., Y. Avraham, and E. M. Berry. 2006. AMPK activation regulates apoptosis, adipogenesis, and lipolysis by eIF2alpha in adipocytes. *Biochem. Biophys. Res. Commun.* **340**: 43–47.
59. Soukas, A., N. D. Socci, B. D. Saatkamp, S. Novelli, and J. M. Friedman. 2001. Distinct transcriptional profiles of adipogenesis in vivo and in vitro. *J. Biol. Chem.* **276**: 34167–34174.
60. Batchvarova, N., X. Z. Wang, and D. Ron. 1995. Inhibition of adipogenesis by the stress-induced protein CHOP (Gadd153). *EMBO J.* **14**: 4654–4661.
61. Shimada, T., N. Hiramatsu, M. Okamura, K. Hayakawa, A. Kasai, J. Yao, and M. Kitamura. 2007. Unexpected blockade of adipocyte differentiation by K-7174: implication for endoplasmic reticulum stress. *Biochem. Biophys. Res. Commun.* **363**: 355–360.
62. Lagace, D. C., and M. W. Nachtigal. 2004. Inhibition of histone deacetylase activity by valproic acid blocks adipogenesis. *J. Biol. Chem.* **279**: 18851–18860.
63. Rubenstein, R. C., and P. L. Zeitlin. 2000. Sodium 4-phenylbutyrate downregulates Hsc70: implications for intracellular trafficking of DeltaF508-CFTR. *Am. J. Physiol. Cell Physiol.* **278**: C259–C267.
64. Iordache, C., and M. Duszyk. 2007. Sodium 4-phenylbutyrate up-regulates ENaC and sodium absorption in T84 cells. *Exp. Cell Res.* **313**: 305–311.
65. Kouraklis, G., and S. Theocharis. 2006. Histone deacetylase inhibitors: a novel target of anticancer therapy (review). *Oncol. Rep.* **15**: 489–494.
66. Fajas, L., V. Egler, R. Reiter, J. Hansen, K. Kristiansen, M. B. Debril, S. Miard, and J. Auwerx. 2002. The retinoblastoma-histone deacetylase

- lase 3 complex inhibits PPARgamma and adipocyte differentiation. *Dev. Cell.* **3**: 903–910.
67. Fu, M., M. Rao, T. Bouras, C. Wang, K. Wu, X. Zhang, Z. Li, T. P. Yao, and R. G. Pestell. 2005. Cyclin D1 inhibits peroxisome proliferator-activated receptor gamma-mediated adipogenesis through histone deacetylase recruitment. *J. Biol. Chem.* **280**: 16934–16941.
 68. Wiper-Bergeron, N., D. Wu, L. Pope, C. Schild-Poulter, and R. J. Hache. 2003. Stimulation of preadipocyte differentiation by steroid through targeting of an HDAC1 complex. *EMBO J.* **22**: 2135–2145.
 69. Yoo, E. J., J. J. Chung, S. S. Choe, K. H. Kim, and J. B. Kim. 2006. Down-regulation of histone deacetylases stimulates adipocyte differentiation. *J. Biol. Chem.* **281**: 6608–6615.
 70. Zuo, Y., L. Qiang, and S. R. Farmer. 2006. Activation of CCAAT/enhancer-binding protein (C/EBP) alpha expression by C/EBP beta during adipogenesis requires a peroxisome proliferator-activated receptor-gamma-associated repression of HDAC1 at the C/ebp alpha gene promoter. *J. Biol. Chem.* **281**: 7960–7967.
 71. Kern, R. M., Z. Yang, P. S. Kim, W. W. Grody, R. K. Iyer, and S. D. Cederbaum. 2007. Arginase induction by sodium phenylbutyrate in mouse tissues and human cell lines. *Mol. Genet. Metab.* **90**: 37–41.
 72. Shack, S., A. Miller, L. Liu, P. Prasanna, A. Thibault, and D. Samid. 1996. Vulnerability of multidrug-resistant tumor cells to the aromatic fatty acids phenylacetate and phenylbutyrate. *Clin. Cancer Res.* **2**: 865–872.
 73. Camacho, L. H., J. Olson, W. P. Tong, C. W. Young, D. R. Spriggs, and M. G. Malkin. 2007. Phase I dose escalation clinical trial of phenylbutyrate sodium administered twice daily to patients with advanced solid tumors. *Invest. New Drugs.* **25**: 131–138.
 74. Sung, M. W., and S. Waxman. 2007. Combination of cytotoxic-differentiation therapy with 5-fluorouracil and phenylbutyrate in patients with advanced colorectal cancer. *Anticancer Res.* **27**: 995–1001.
 75. Caruthers, R. L., and C. E. Johnson. 2007. Stability of extemporaneously prepared sodium phenylbutyrate oral suspensions. *Am. J. Health Syst. Pharm.* **64**: 1513–1515.
 76. Hines, P., G. J. Dover, and L. M. Resar. 2008. Pulsed-dosing with oral sodium phenylbutyrate increases hemoglobin F in a patient with sickle cell anemia. *Pediatr. Blood Cancer.* **50**: 357–359.
 77. Phuphanich, S., S. D. Baker, S. A. Grossman, K. A. Carson, M. R. Gilbert, J. D. Fisher, and M. A. Carducci. 2005. Oral sodium phenylbutyrate in patients with recurrent malignant gliomas: a dose escalation and pharmacologic study. *Neuro-oncol.* **7**: 177–182.
 78. Resar, L. M., J. B. Segal, L. K. Fitzpatrick, A. Friedmann, S. W. Brusilow, and G. J. Dover. 2002. Induction of fetal hemoglobin synthesis in children with sickle cell anemia on low-dose oral sodium phenylbutyrate therapy. *J. Pediatr. Hematol. Oncol.* **24**: 737–741.
 79. Colgan, S. M., D. Tang, G. H. Werstuck, and R. C. Austin. 2007. Endoplasmic reticulum stress causes the activation of sterol regulatory element binding protein-2. *Int. J. Biochem. Cell Biol.* **39**: 1843–1851.
 80. Wang, H., G. Kouri, and C. B. Wollheim. 2005. ER stress and SREBP-1 activation are implicated in beta-cell glucolipotoxicity. *J. Cell Sci.* **118**: 3905–3915.
 81. Kammoun, H. L., H. Chabanon, I. Hainault, S. Luquet, C. Magnan, T. Koike, P. Ferre, and F. Foufelle. 2009. GRP78 expression inhibits insulin and ER stress-induced SREBP-1c activation and reduces hepatic steatosis in mice. *J. Clin. Invest.* **119**: 1201–1215.